Chin. Phys. B Vol. 29, No. 3 (2020) 030201

Lump and interaction solutions to the (3+1)-dimensional Burgers equation*

Jian Liu(刘健)[1,†] and Jian-Wen Wu(吴剑文)[2]

[1] *Department of Mathematics and Physics, Quzhou University, Quzhou 324000, China*
[2] *Department of Physics, Zhejiang Normal University, Jinhua 321004, China*

(Received 6 November 2019; revised manuscript received 27 December 2019; accepted manuscript online 9 January 2020)

The (3+1)-dimensional Burgers equation, which describes nonlinear waves in turbulence and the interface dynamics, is considered. Two types of semi-rational solutions, namely, the lump–kink solution and the lump–two kinks solution, are constructed from the quadratic function ansatz. Some interesting features of interactions between lumps and other solitons are revealed analytically and shown graphically, such as fusion and fission processes.

Keywords: (3+1)-dimensional Burgers equation, lump solution, interaction wave solution, bilinear form

PACS: 02.30.Jr, 02.70.Wz, 02.60.Cb **DOI:** 10.1088/1674-1056/ab6964

1. Introduction

The balance between nonlinearity and dispersion leads to various localized waves. Among them, soliton is a classic type of nonlinear wave which preserves its shape during space–time evolution. It arises as a fundamental phenomenon in diverse physical systems, such as plasma physics, nonlinear optics, and hydrodynamics.[1] Unlike solitons localized in certain direction, lumps are rational function solutions localized in all directions in space.[2] Systems in which lumps occur include the ferromagnetic slab,[3] supermembrane,[4] and thin fluid layer.[5] Recently, the study of lump solution to nonlinear partial differential equations has attracted more and more attention. Based on the Hirota bilinear formulation, lump solutions to the integrable systems are obtained from the quadratic functions ansatz, such as the Kadomtsev–Petviashvili (KP) equation,[6] the generalized KP equation,[7] and the Sawada–Kotera equation.[8] Hinted by these results, a wide diversity of interaction solutions between lumps and other types of solitons are studied by combining an exponential function in quadratic functions.[9–22]

This work deals with the well-known (3+1)-dimensional Burgers (3DBG) system[23–25]

$$
\begin{aligned}
&u_t=\alpha(u_{xx}+2vu_x)+\beta(u_{yy}+2uu_y)+\gamma(u_{zz}+2wu_z),\\
&u_x=v_y,\\
&u_z=w_y,
\end{aligned}
\tag{1}
$$

which describes the propagation of nonlinear waves in turbulence and the interface dynamics.[23] The elastic interactions among different types of nonlinear waves, such as the embedded ring-soliton on a periodic wave background, are studied by using the modified mapping method.[23] Furthermore, abundant localized excitations in (3+1)-dimensions, such as the paraboloid-type camber soliton and a dipole type dromion, are revealed via the multi-linear variable separation approach.[24] Obviously, if u is z independent, the system (1) will degenerate to the known (2+1)-dimensional Burgers equation.[26,27]

This paper is organized as follows. In the next section, the lump solution of the 3DBG system is obtained by applying a direct method based on Hirota bilinear formulation. In Section 3, the interaction solution between one lump and a single kink are obtained by adding an exponential function in the quadratic function. The second type of semi-rational solution, which contains the lump and the coupled stripe soliton pair, is revealed in Section 4. The last section gives a short summary and discussion.

2. Lump solution

The 3DBG system (1) can be transformed to the following Hirota bilinear form:

$$
\begin{aligned}
&ff_{yt}-f_yf_t+\alpha\,[f_yf_{xx}-ff_{xxy}+2v_0(f_xf_y-ff_{xy})]\\
&+\beta\,[f_yf_{yy}-ff_{yyy}+2u_0(f_y^2-ff_{yy})]\\
&+\gamma[f_yf_{zz}-ff_{yzz}+2w_0(f_yf_z-ff_{yz})]=0,
\end{aligned}
\tag{2}
$$

through the Cole–Hopf transformation

$$
u=(\ln f)_y+u_0,\quad v=(\ln f)_x+v_0,\quad w=(\ln f)_z+w_0,
\tag{3}
$$

where u_0, v_0, and w_0 are real constants.

In order to construct lump solutions to the 3DBG system (1), we assume that the function f takes the following quadratic form:

$$
\begin{aligned}
&f=g^2+h^2+a_{11},\\
&g=a_1x+a_2y+a_3z+a_4t+a_5,
\end{aligned}
$$

*Project supported by the National Natural Science Foundation of China (Grant Nos. 11501323, 11701323, and 11605102).
†Corresponding author. E-mail: jian.liu_math@qzc.edu.cn
 http://iopscience.iop.org/cpb http://cpb.iphy.ac.cn

$$h = a_6x + a_7y + a_8z + a_9t + a_{10}, \tag{4}$$

where a_i $(i = 1, 2, \ldots, 11)$ are the real parameters to be determined later. Substituting Eq. (4) into the bilinear equation (2) and setting to zero all the coefficients of the space–time variables x, y, z, and t, we obtain a set of algebraic equations in a_i. Solving these equations yields many classes of solutions, we choose the following one with the least parameters determined:

$$\begin{aligned} &a_1 = \sqrt{-A/\alpha}, \quad a_4 = \alpha v_0 a_1 + \beta u_0 a_2 + \gamma w_0 a_3, \\ &a_9 = \alpha v_0 a_6 + \beta u_0 a_7 + \gamma w_0 a_8, \\ &A = [\alpha a_6^2 + \beta(a_2^2 + a_7^2) + \gamma(a_3^2 + a_8^2)]. \end{aligned} \tag{5}$$

Obviously, the parameters $\{a_2, a_3, a_5, a_6, a_7, a_8, a_{10}, a_{11}\}$ are left as arbitrary and $\{a_4, a_9\}$ are relevant to the seed solution $\{u_0, v_0, w_0\}$.

By using the transformation (3), the explicit solution of system (1) in rational form can be expressed as

$$\begin{aligned} &u = \frac{2(a_2g + a_7h)}{g^2 + h^2 + a_{11}} + u_0, \quad v = \frac{2(a_1g + a_6h)}{g^2 + h^2 + a_{11}} + v_0, \\ &w = \frac{2(a_3g + a_8h)}{g^2 + h^2 + a_{11}} + w_0, \end{aligned} \tag{6}$$

where

$$\begin{aligned} g &= \sqrt{-A/\alpha}x + a_2y + a_3z \\ &\quad + \left(\alpha v_0\sqrt{-A/\alpha} + \beta u_0 a_2 + \gamma w_0 a_3\right)t + a_5, \\ h &= a_6x + a_7y + a_8z + (\alpha v_0 a_6 + \beta u_0 a_7 + \gamma w_0 a_8)t + a_{10}. \end{aligned}$$

To ensure the solution (6) rationally localized in all directions in space, one notes that the constant a_1 in Eq. (5) must be real and postive. Hence, we introduce the constraint condition

$$\alpha A = \alpha[\alpha a_6^2 + \beta(a_2^2 + a_7^2) + \gamma(a_3^2 + a_8^2)] < 0.$$

Now, let us analyze the characteristics of space–time evolution of the lump structure. For simplicity, we take the lump solution u in x–y plane with $z = 0$ as an example. The location of a lump solution is defined at the point where the max $|u|$ is attained and can be traced out by assuming the partial derivatives u_x and u_y to be zero. From $u_x = u_y = 0$, it is found that the extreme values locate at the two critical points

$$\begin{aligned} &\left[\frac{(a_2a_9 - a_4a_7)t + (a_2a_{10} - a_5a_7)}{a_1a_7 - a_2a_6},\right. \\ &\frac{(a_4a_6 - a_1a_9)t + (a_5a_6 - a_1a_{10})}{a_1a_7 - a_2a_6} \\ &\left.\pm\sqrt{\frac{(a_1a_7 - a_2a_6)^2 a_{11}}{a_2^2 + a_7^2}}\right]. \end{aligned} \tag{7}$$

Choosing $u_0 = 0$, the amplitude of u is

$$|u|_{\max} = \sqrt{\frac{(a_2^2 + a_7^2)(a_1a_7 - a_2a_6)^2}{a_{11}[1 + (a_1a_7 - a_2a_6)^2]}}. \tag{8}$$

From Eq. (7), we know that the lump peak/valley moves along the route line

$$\begin{aligned} y &= \frac{a_4a_6 - a_1a_9}{a_2a_9 - a_4a_7}x + \frac{a_4a_{10} - a_5a_9}{a_2a_9 - a_4a_7} \\ &\quad \pm\sqrt{\frac{(a_1a_7 - a_2a_6)^2 a_{11}}{a_2^2 + a_7^2}}, \end{aligned} \tag{9}$$

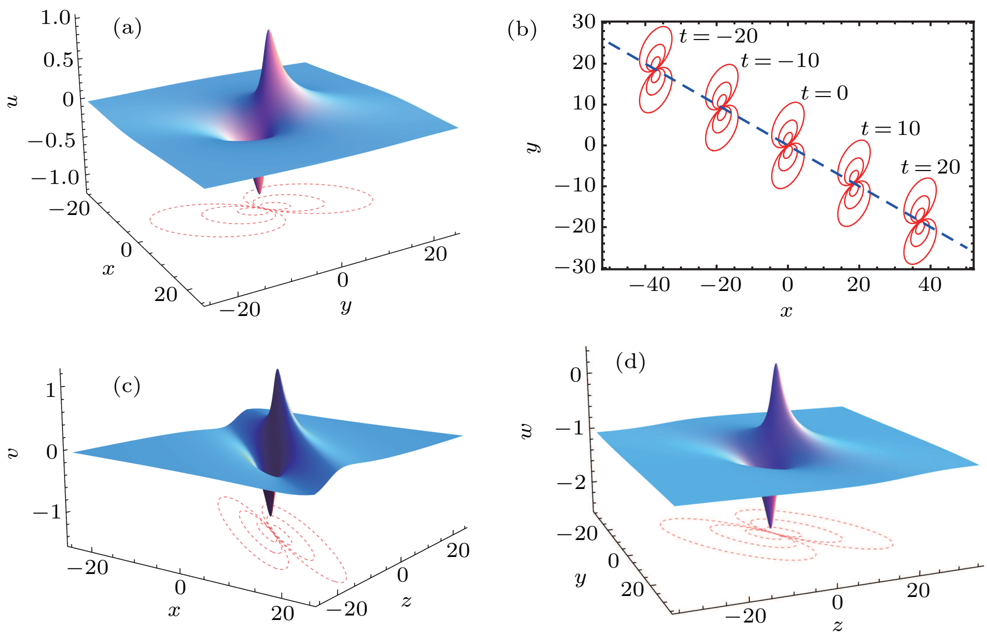

Fig. 1. Plots of the lump structures in solution (6) with parameters $\alpha = -2$, $\beta = \gamma = a_3 = -w_0 = 1$, $-a_2 = a_7 = a_{11} = 0.5$, $a_5 = a_{10} = u_0 = v_0 = 0$, and $a_6 = 0.25$. (a) The three-dimensional plot of u. (b) The contour plot of u in x–y plane at different time. (c) The three-dimensional plot of v. (d) The three-dimensional plot of w.

which implies that the lump's peak and valley are symmetric to each other with respect to the straight line $y = [(a_4a_6 - a_1a_9)x + (a_4a_{10} - a_5a_9)]/(a_2a_9 - a_4a_7)$. To illustrate the lump structure more clearly, let us look at some figures. Figure 1(a) exhibits the three-dimensional lump structure of solution u in x–y plane with $z = t = 0$. From Eq. (8), the amplitude of u can be approximately calculated as 0.836 which is in accordance with the figure. Figure 1(b) shows the contour plots of u at different time. It is obvious that the locations of lump's peak and valley are symmetric to the straight line $y = -x/2$. Figure 1(c) shows the lump structure v in x–z plane with $y = t = 0$. Figure 1(d) displays the lump structure of w in y–z plane with $x = t = 0$ on a constant background $w_0 = -1$.

3. Lump interacting with one stripe soliton

As is well known, one can always take the function f in the exponential form to obtain single or multiple soliton solutions. Based on this fact, the exponential function is added to quadratic function f, which reads

$$\begin{aligned} f &= g^2 + h^2 + a_{11}\,\mathrm{e}^{\xi} + a_{12}, \\ g &= a_1x + a_2y + a_3z + a_4t + a_5, \\ h &= a_6x + a_7y + a_8z + a_9t + a_{10}, \\ \xi &= k_1x + k_2y + k_3z + \omega t, \end{aligned} \tag{10}$$

with a_i, k_i, and ω being real parameters to be determined later. Substituting Eq. (10) into the bilinear equation (2) yields, after elimination of the coefficients of polynomials x, y, z, and t, a set of more algebraic equations. From these equations, a nontrivial solution of four wave parameters $\{a_1, a_4, a_9, \omega\}$ can be determined as

$$\begin{aligned} a_1 &= \sqrt{-A/\alpha}, \quad a_4 = \alpha v_0 a_1 + \beta u_0 a_2 + \gamma w_0 a_3, \\ a_9 &= \alpha v_0 a_6 + \beta u_0 a_7 + \gamma w_0 a_8, \\ \omega &= \alpha(k_1^2 + v_0k_1) + \beta(k_2^2 + u_0k_2) + \gamma(k_3^2 + w_0k_3), \\ A &= [\alpha a_6^2 + \beta(a_2^2 + a_7^2) + \gamma(a_3^2 + a_8^2)]. \end{aligned} \tag{11}$$

The expression of a_1 leads to the constraint condition $\alpha[\alpha a_6^2 + \beta(a_2^2 + a_7^2) + \gamma(a_3^2 + a_8^2)] < 0$. Through the transformation (3), the lump-kink solution of the 3DBG system (1) is obtained as

$$\begin{aligned} u &= \frac{2(a_2g + a_7h) + a_{11}k_2\,\mathrm{e}^{\xi}}{g^2 + h^2 + a_{11}\,\mathrm{e}^{\xi} + a_{12}} + u_0, \\ v &= \frac{2(a_1g + a_6h) + a_{11}k_1\,\mathrm{e}^{\xi}}{g^2 + h^2 + a_{11}\,\mathrm{e}^{\xi} + a_{12}} + v_0, \\ w &= \frac{2(a_3g + a_8h) + a_{11}k_3\,\mathrm{e}^{\xi}}{g^2 + h^2 + a_{11}\,\mathrm{e}^{\xi} + a_{12}} + w_0, \end{aligned} \tag{12}$$

where

$$\begin{aligned} g &= \sqrt{-A/\alpha}x + a_2y + a_3z \\ &\quad + (\alpha v_0\sqrt{-A/\alpha} + \beta u_0a_2 + \gamma w_0a_3)t + a_5, \\ h &= a_6x + a_7y + a_8z + (\alpha v_0a_6 + \beta u_0a_7 + \gamma w_0a_8,)t + a_{10}, \\ \xi &= k_1x + k_2y + k_3z + [\alpha(k_1^2 + v_0k_1) \\ &\quad + \beta(k_2^2 + u_0k_2) + \gamma(k_3^2 + w_0k_3)]t. \end{aligned} \tag{13}$$

The semi-rational solution (12) describes the interaction between the lump and one stripe soliton due to the appearance of both exponential terms and quadratic functions. Its asymptotic behaviors of propagation implies two types of interesting nonlinear phenomena, namely, fusion and fission. To figure out this, we take u in solution (12) as an example, with the assumption that x, y, and z are constants and $\omega < 0$. As $t \to -\infty$, it is obvious that the exponential term e^{ξ} is the dominant one and $u \to u_0 + k_2$, which exclude the existence of lump structure. On the contrary, the rational function $g^2 + h^2 + a_{12}$ is the dominant term and $u \to u_0 + 2(a_2g + a_7h)/(g^2 + h^2 + a_{12})$ as $t \to +\infty$. The whole process is the fission phenomenon as presented in Fig. 2 with $\omega = -0.09 < 0$. At time $t = -100$, only the single-kink structure can be observed in Fig. 2(a). As time approaches zero, the lump structure trends to appear and thrive. In Fig. 2(b), one can observe that one stripe soliton has split into one lump structure and one kink soliton at time $t = 0$. Figure 2(c) shows that the lump structure tends to depart from the soliton line as time goes on. Figure 3 is the corresponding contour plot. One can also observe the fusion process with parameters $\alpha = a_{12} = 2$, $\beta = \gamma = -1$, $a_2 = a_7 = 0.25$, $a_3 = -a_6 = a_8 = 0.5$, $a_5 = a_{10} = u_0 = v_0 = k_3 = 0$, $a_{11} = w_0 = 1$, and $k_1 = k_2 = 0.3$. Here we omit the plot.

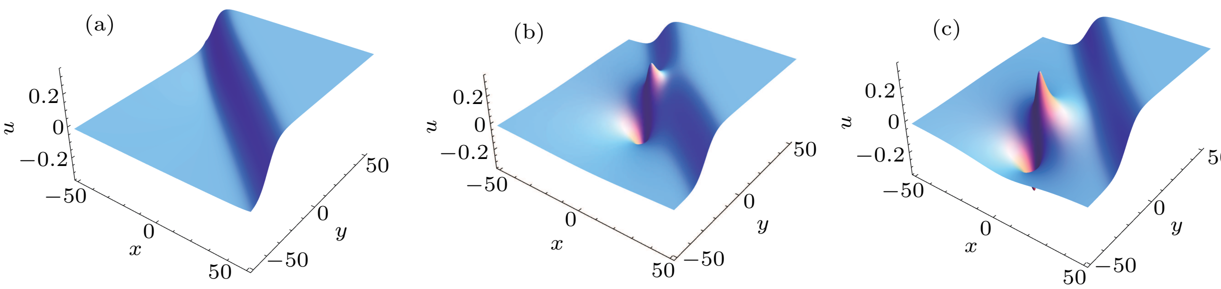

Fig. 2. The three-dimensional plots of the lump–kink solution u in Eq. (12) with $z = 0$ at different time: (a) $t = -50$, (b) $t = 0$, (c) $t = 20$. The free parameters are select as $-\alpha = a_{12} = 2$, $\beta = \gamma = a_{11} = w_0 = 1$, $-a_2 = k_1 = k_2 = 0.3$, $-a_3 = a_6 = a_7 = 0.4$, and $a_5 = a_{10} = u_0 = v_0 = k_3 = 0$.

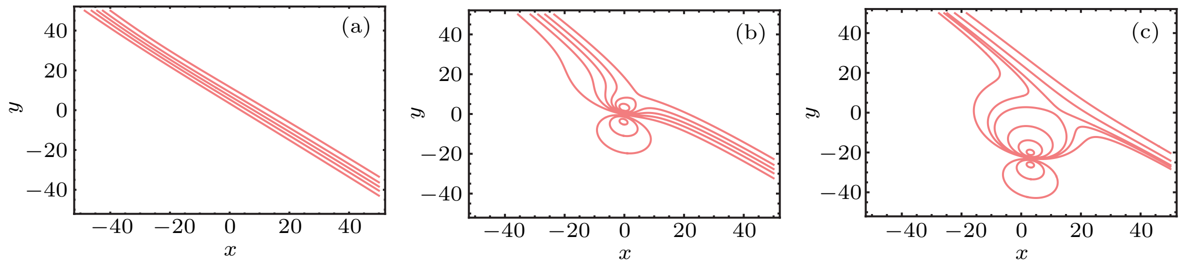

Fig. 3. The contour plots of the lump-kink solution u in Eq. (12) with $z=0$ at different time. The free parameters selection are the same as Fig. 2. (a) $t=-50$; (b) $t=0$; (c) $t=20$.

4. Interaction between the lump and a pair of stripe solitons

In this section, we focus on the interaction solution between the lump and a pair of stripe solitons. To this end, we assume

$$\begin{aligned} f &= g^2+h^2+a_{11}\,\mathrm{e}^{\xi}+a_{12}\,\mathrm{e}^{-\xi}+a_{13}, \\ g &= a_1x+a_2y+a_3z+a_4t+a_5, \\ h &= a_6x+a_7y+a_8z+a_9t+a_{10}, \\ \xi &= k_1x+k_2y+k_3z+\omega t, \end{aligned} \tag{14}$$

where the real parameters a_i, k_i, and ω are to be determined later. Substituting Eq. (14) into Eq. (2) and proceeding as in the previous section, we obtain a nontrivial solution of five determined wave parameters $\{a_1,a_4,a_9,k_1,\omega\}$

$$\begin{aligned} & a_1=\sqrt{-A/\alpha}, \quad a_4=\alpha v_0a_1+\beta u_0a_2+\gamma w_0a_3, \\ & a_9=\alpha v_0a_6+\beta u_0a_7+\gamma w_0a_8, \\ & k_1=\sqrt{-\frac{\beta k_2^2+\gamma k_3^2}{\alpha}}, \quad \omega=\alpha v_0k_1+\beta u_0k_2+\gamma w_0k_3, \end{aligned}$$

$$A=[\alpha a_6^2+\beta(a_2^2+a_7^2)+\gamma(a_3^2+a_8^2)], \tag{15}$$

with constraint conditions $\alpha[\alpha a_6^2+\beta(a_2^2+a_7^2)+\gamma(a_3^2+a_8^2)]<0$ and $\alpha[\beta k_2^2+\gamma k_3^2]<0$.

Using the transformation (3), we have the following explicit interaction solution to the 3DBG system (1):

$$\begin{aligned} u &= \frac{2(a_2g+a_7h)+k_2(a_{11}\,\mathrm{e}^{\xi}-a_{12}\,\mathrm{e}^{-\xi})}{g^2+h^2+a_{11}\,\mathrm{e}^{\xi}+a_{12}\,\mathrm{e}^{-\xi}+a_{13}}+u_0, \\ v &= \frac{2(a_1g+a_6h)+k_1(a_{11}\,\mathrm{e}^{\xi}-a_{12}\,\mathrm{e}^{-\xi})}{g^2+h^2+a_{11}\,\mathrm{e}^{\xi}+a_{12}\,\mathrm{e}^{-\xi}+a_{13}}+v_0, \\ w &= \frac{2(a_3g+a_8h)+k_3(a_{11}\,\mathrm{e}^{\xi}-a_{12}\,\mathrm{e}^{-\xi})}{g^2+h^2+a_{11}\,\mathrm{e}^{\xi}+a_{12}\,\mathrm{e}^{-\xi}+a_{13}}+w_0, \end{aligned} \tag{16}$$

where

$$\begin{aligned} g &= \sqrt{-A/\alpha}x+a_2y+a_3z \\ &\quad +(\alpha v_0\sqrt{-A/\alpha}+\beta u_0a_2+\gamma w_0a_3)t+a_5, \\ h &= a_6x+a_7y+a_8z+(\alpha v_0a_6+\beta u_0a_7+\gamma w_0a_8)t+a_{10}, \\ \xi &= \sqrt{-\frac{\beta k_2^2+\gamma k_3^2}{\alpha}}x+k_2y+k_3z+(\alpha v_0k_1+\beta u_0k_2+\gamma w_0k_3)t. \end{aligned}$$

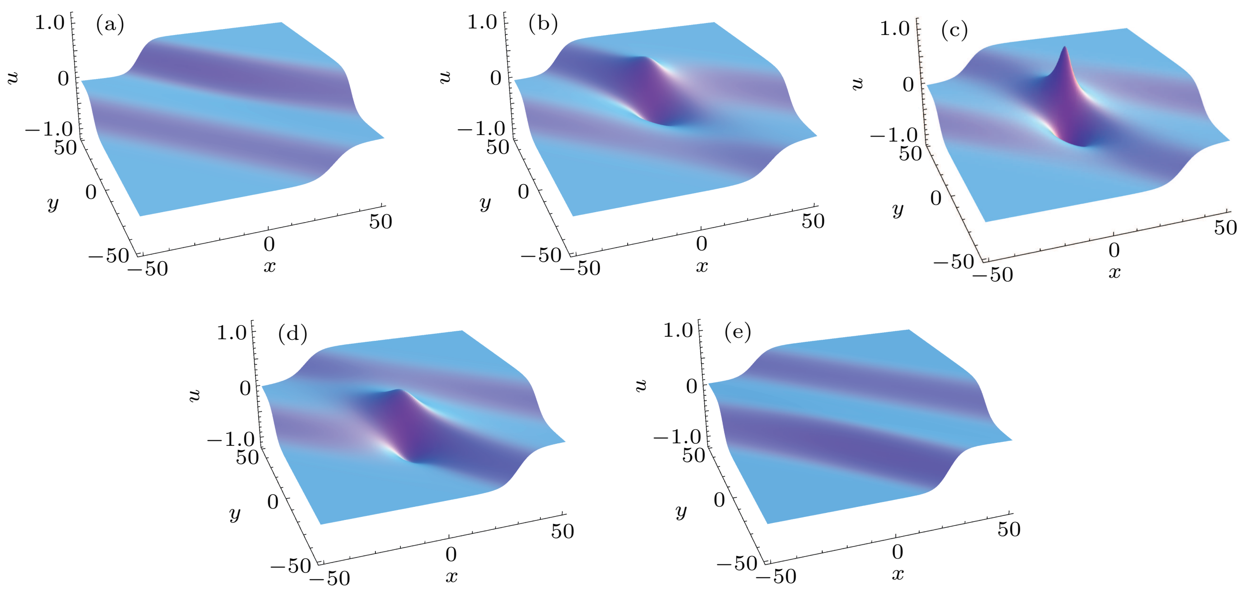

Fig. 4. The three-dimensional plots of the lump–two kinks solution u in Eq. (16) with $z=0$ at different time: (a) $t=-25$, (b) $t=-5$, (c) $t=0$, (d) $t=5$, (e) $t=25$. The free parameters are selected as $\alpha=a_{11}=a_{12}=1$, $\beta=\gamma=w_0=-1$, $a_2=a_3=a_7=a_8=v_0=0.5$, $a_5=a_{10}=a_{13}=u_0=k_3=0$, and $a_6=0.1$.

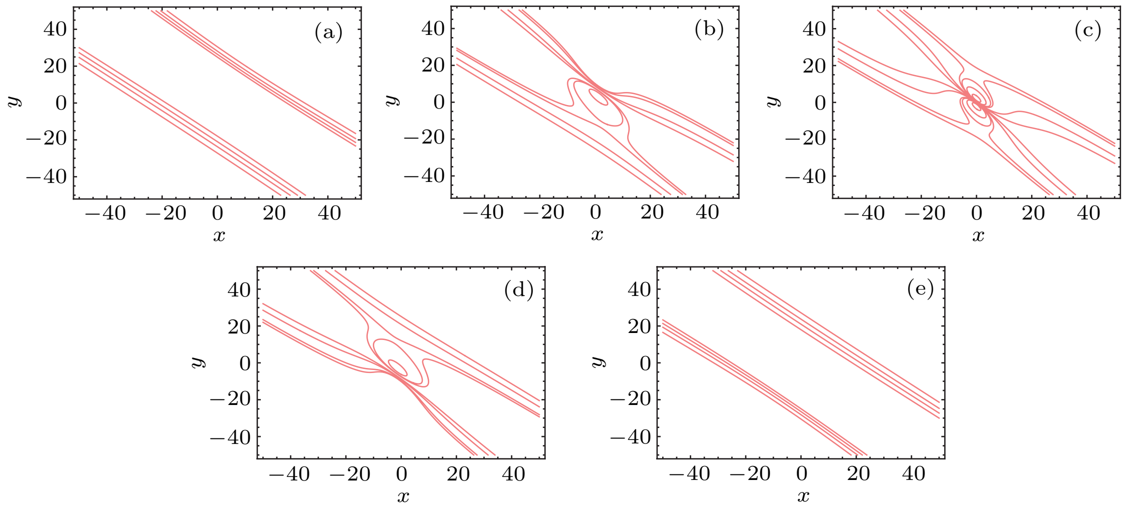

Fig. 5. The contour plots of the lump–two kinks solution u in Eq. (16) with $z=0$ at different time: (a) $t=-25$, (b) $t=-5$, (c) $t=0$, (d) $t=-5$, (e) $t=25$. The free parameters are the same as those in Fig. 4.

The semi-rational solution (16) depicts the interactions between the lump and a pair of stripe solitons. Then, some interesting asymptotic behaviors of the solution should be pointed out. Similarly, we take the solution u as an example. As $t \to \pm\infty$, the solution u approaches the resonant stripe soliton limit[28]

$$u = \frac{k_2(a_{11}\,\mathrm{e}^{\xi} - a_{12}\,\mathrm{e}^{-\xi})}{(a_4^2 + a_9^2)t^2 + a_{11}\,\mathrm{e}^{\xi} + a_{12}\,\mathrm{e}^{-\xi}} + u_0, \tag{17}$$

while for $t \to 0$, the rational lump thrives and attains its peak. Such kind phenomenon is illustrated in Figs. 4 and 5 by giving three-dimensional and corresponding contour plots.

5. Discussion and conclusion

In this work, the 3DBG system is studied by employing a direct method based on Hirota bilinear formulation. The lump solution and two types of semi-rational solutions are obtained from the quadratic function ansatz. Some interesting features of wave interaction are revealed. The first type of semi-rational solution describes the interaction between the lump and one stripe soliton, which leads to two opposite processes of fission and fusion. The second type of semi-rational solution contains the lump and the coupled stripe soliton pair. As shown in Figs. 4 and 5, one can observe that a lump arises from the resonant stripe soliton and is swallowed by it finally. It is hoped that the result can be helpful for understanding nonlinear waves in turbulence and interface dynamics.

References

[1] Dauxois T and Peyrard M 2006 *Physics of Solitons* (Cambridge: Cambridge Univ. Press)
[2] Manakov S V, Zakhorov V E and Bordag L A 1977 *Phys. Lett.* **63** 205
[3] Leblond H and Manna M 2007 *Phys. Rev. Lett.* **99** 064102
[4] Bergshoeff E and Townsend P K 1999 *J. High Energy Phys.* **9905** 021
[5] Falcon E, Laroche C and Fauve S 2002 *Phys. Rev. Lett.* **89** 204501
[6] Ma W X 2015 *Phys. Lett. A* **379** 1975
[7] Ma W X and Zhou Y 2017 *J. Differential Equations* **264** 2633
[8] Zhang H Q and Ma W X 2018 *Nonlinear Dyn.***87** 2305
[9] Guo F and Lin J 2019 *Nonlinear Dyn.* **96** 1233
[10] Ren B, Ma W X and Yu J 2019 *Comput. Math. Appl.***77** 2086
[11] Yang Y Q, Wang X and Cheng X P 2018 *Wave Motion* **77** 1
[12] Hao X Z, Liu Y P, Li Z B and Ma W X 2019 *Comput. Math. Appl.* **77** 724
[13] Yang Y Q, Yan Z Y and Malomed B A 2015 *Chaos* **25** 103112
[14] Wang X B, Tian S F, Qin C Y and Zhang T T 2017 *Appl. Math. Lett.* **68** 40
[15] Ren B, Ma W X and Yu J 2019 *Nonlinear Dyn.* **96** 717
[16] Tang Y N, Tao S Q, Zhou M L and Guan Q 2017 *Nonlinear Dyn.* **89** 429
[17] Liu J G and He Y 2018 *Nonlinear Dyn.* **92** 1103
[18] Ma W X, Yong X L and Zhang H Q 2018 *Comput. Math. Appl.* **75** 289
[19] Lou S Y and Lin J 2018 *Chin. Phys. Lett.* **35** 050202
[20] Kofane T C, Fokou M, Mohamadou A and Yomba E 2017 *Eur. Phys. J. Plus* **132** 465
[21] An H L, Feng D and Zhu H X 2019 *Nonlinear Dyn.* **98** 1275
[22] Li W T, Zhang Z, Yang X Y and Li B 2019 *Int. J. Mod. Phys. B* **22** 1950255
[23] Dai C Q and Wang Y Y 2009 *Phys. Lett. A* **373** 181
[24] Yin J P and Lou S Y 2003 *Chin. Phys. Lett.* **20** 1448
[25] Dai C Q and Yu F B 2014 *Wave Motion* **51** 52
[26] Tang X Y and Lou S Y 2003 *Chin. Phys. Lett.* **20** 335
[27] Wang H 2018 *Appl. Math. Lett.* **85** 27
[28] Wang S, Tang X Y and Lou S Y 2004 *Chaos Solitons Fract.* **21** 231